

Comparison of the space-time extent of the pion emission source in $d+Au$ and $Au+Au$ collisions at $\sqrt{s_{NN}} = 200$ GeV

A. Adare,¹³ S. Afanasiev,³² C. Aidala,^{45,46} N.N. Ajitanand,⁶⁴ Y. Akiba,^{58,59} R. Akimoto,¹² H. Al-Bataineh,⁵² J. Alexander,⁶⁴ M. Alfred,²⁵ A. Angerami,¹⁴ K. Aoki,^{37,58} N. Apadula,⁶⁵ Y. Aramaki,^{12,58} H. Asano,^{37,58} E.T. Atomssa,^{38,65} R. Averbek,⁶⁵ T.C. Awes,⁵⁴ B. Azmoun,⁷ V. Babintsev,²⁶ M. Bai,⁶ G. Baksay,²⁰ L. Baksay,²⁰ N.S. Bandara,⁴⁵ B. Bannier,⁶⁵ K.N. Barish,⁸ B. Bassalleck,⁵¹ A.T. Basye,¹ S. Bathe,^{5,8,59} V. Baublis,⁵⁷ C. Baumann,⁴⁷ A. Bazilevsky,⁷ M. Beaumier,⁸ S. Beckman,¹³ S. Belikov,^{7,*} R. Belmont,^{46,69} R. Bennett,⁶⁵ A. Berdnikov,⁶¹ Y. Berdnikov,⁶¹ J.H. Bhom,⁷³ A.A. Bickley,¹³ D. Black,⁸ D.S. Blau,³⁶ J. Bok,⁵² J.S. Bok,⁷³ K. Boyle,^{59,65} M.L. Brooks,⁴¹ J. Bryslawskyj,⁵ H. Buesching,⁷ V. Bumazhnov,²⁶ G. Bunce,^{7,59} S. Butsyk,⁴¹ C.M. Camacho,⁴¹ S. Campbell,^{30,65} A. Caringi,⁴⁸ C.-H. Chen,^{59,65} C.Y. Chi,¹⁴ M. Chiu,⁷ I.J. Choi,^{27,73} J.B. Choi,¹⁰ R.K. Choudhury,⁴ P. Christiansen,⁴³ T. Chujo,⁶⁸ P. Chung,⁶⁴ O. Chvala,⁸ V. Cianciolo,⁵⁴ Z. Citron,^{65,71} B.A. Cole,¹⁴ Z. Conesa del Valle,³⁸ M. Connors,⁶⁵ P. Constantin,⁴¹ M. Csanád,¹⁸ T. Csörgő,⁷² T. Dahms,⁶⁵ S. Dairaku,^{37,58} I. Danchev,⁶⁹ K. Das,²¹ A. Datta,^{45,51} M.S. Daugherty,¹ G. David,⁷ M.K. Dayananda,²² K. DeBlasio,⁵¹ K. Dehmelt,⁶⁵ A. Denisov,²⁶ A. Deshpande,^{59,65} E.J. Desmond,⁷ K.V. Dharmawardane,⁵² O. Dietzsch,⁶² L. Ding,³⁰ A. Dion,^{30,65} J.H. Do,⁷³ M. Donadelli,⁶² O. Drapier,³⁸ A. Drees,⁶⁵ K.A. Drees,⁶ J.M. Durham,^{41,65} A. Durum,²⁶ D. Dutta,⁴ L. D’Orazio,⁴⁴ S. Edwards,²¹ Y.V. Efremenko,⁵⁴ F. Ellinghaus,¹³ T. Engelmores,¹⁴ A. Enokizono,^{40,54,58,60} H. En’yo,^{58,59} S. Esumi,⁶⁸ B. Fadem,⁴⁸ N. Feege,⁶⁵ D.E. Fields,⁵¹ M. Finger,⁹ M. Finger, Jr.,⁹ F. Fleuret,³⁸ S.L. Fokin,³⁶ Z. Fraenkel,^{71,*} J.E. Frantz,^{53,65} A. Franz,⁷ A.D. Frawley,²¹ K. Fujiwara,⁵⁸ Y. Fukao,⁵⁸ T. Fusayasu,⁵⁰ C. Gal,⁶⁵ P. Gallus,¹⁵ P. Garg,³ I. Garishvili,⁶⁶ H. Ge,⁶⁵ F. Giordano,²⁷ A. Glenn,^{13,40} H. Gong,⁶⁵ M. Gonin,³⁸ Y. Goto,^{58,59} R. Granier de Cassagnac,³⁸ N. Grau,^{2,14} S.V. Greene,⁶⁹ G. Grim,⁴¹ M. Grosse Perdekamp,^{27,59} Y. Gu,⁶⁴ T. Gunji,¹² H. Guragain,²² H.-Å. Gustafsson,^{43,*} T. Hachiya,⁵⁸ J.S. Haggerty,⁷ K.I. Hahn,¹⁹ H. Hamagaki,¹² J. Hamblen,⁶⁶ R. Han,⁵⁶ S.Y. Han,¹⁹ J. Hanks,^{14,65} E.P. Hartouni,⁴⁰ S. Hasegawa,³¹ E. Haslum,⁴³ R. Hayano,¹² X. He,²² M. Heffner,⁴⁰ T.K. Hemmick,⁶⁵ T. Hester,⁸ J.C. Hill,³⁰ M. Hohlmann,²⁰ R.S. Hollis,⁸ W. Holzmann,¹⁴ K. Homma,²⁴ B. Hong,³⁵ T. Horaguchi,²⁴ D. Hornback,⁶⁶ T. Hoshino,²⁴ J. Huang,^{7,41} S. Huang,⁶⁹ T. Ichihara,^{58,59} R. Ichimiya,⁵⁸ J. Ide,⁴⁸ Y. Ikeda,^{58,68} K. Imai,^{31,37,58} Y. Imazu,⁵⁸ M. Inaba,⁶⁸ A. Iordanova,⁸ D. Isenhower,¹ M. Ishihara,⁵⁸ T. Isobe,^{12,58} M. Issah,⁶⁹ A. Isupov,³² D. Ivanischev,⁵⁷ D. Ivanishchev,⁵⁷ Y. Iwanaga,²⁴ B.V. Jacak,⁶⁵ S.J. Jeon,⁴⁹ M. Jezghani,²² J. Jia,^{7,64} X. Jiang,⁴¹ J. Jin,¹⁴ B.M. Johnson,⁷ T. Jones,¹ E. Joo,³⁵ K.S. Joo,⁴⁹ D. Jouan,⁵⁵ D.S. Jumper,^{1,27} F. Kajihara,¹² S. Kametani,⁵⁸ N. Kamihara,⁵⁹ J. Kamin,⁶⁵ J.H. Kang,⁷³ J.S. Kang,²³ J. Kapustinsky,⁴¹ K. Karatsu,^{37,58} M. Kasai,^{58,60} D. Kawall,^{45,59} M. Kawashima,^{58,60} A.V. Kazantsev,³⁶ T. Kempel,³⁰ J.A. Key,⁵¹ V. Khachatryan,⁶⁵ A. Khanzadeev,⁵⁷ K. Kihara,⁶⁸ K.M. Kijima,²⁴ J. Kikuchi,⁷⁰ A. Kim,¹⁹ B.I. Kim,³⁵ C. Kim,³⁵ D.H. Kim,^{19,49} D.J. Kim,³³ E. Kim,⁶³ E.-J. Kim,¹⁰ H.-J. Kim,⁷³ M. Kim,⁶³ S.H. Kim,⁷³ Y.-J. Kim,²⁷ Y.K. Kim,²³ E. Kinney,¹³ K. Kiriluk,¹³ Á. Kiss,¹⁸ E. Kistenev,⁷ J. Klatsky,²¹ D. Kleinjan,⁸ P. Kline,⁶⁵ T. Koblesky,¹³ L. Kochenda,⁵⁷ M. Kofarago,¹⁸ B. Komkov,⁵⁷ M. Konno,⁶⁸ J. Koster,^{27,59} D. Kotchetkov,⁵¹ D. Kotov,^{57,61} A. Kozlov,⁷¹ A. Král,¹⁵ A. Kravitz,¹⁴ G.J. Kunde,⁴¹ K. Kurita,^{58,60} M. Kurosawa,^{58,59} Y. Kwon,⁷³ G.S. Kyle,⁵² R. Lacey,⁶⁴ Y.S. Lai,¹⁴ J.G. Lajoie,³⁰ A. Lebedev,³⁰ D.M. Lee,⁴¹ J. Lee,¹⁹ K. Lee,⁶³ K.B. Lee,^{35,41} K.S. Lee,³⁵ S.H. Lee,⁶⁵ M.J. Leitch,⁴¹ M.A.L. Leite,⁶² M. Leitgab,²⁷ E. Leitner,⁶⁹ B. Lenzi,⁶² X. Li,¹¹ P. Lichtenwalner,⁴⁸ P. Liebing,⁵⁹ S.H. Lim,⁷³ L.A. Linden Levy,¹³ T. Liška,¹⁵ A. Litvinenko,³² H. Liu,^{41,52} M.X. Liu,⁴¹ B. Love,⁶⁹ R. Luechtenborg,⁴⁷ D. Lynch,⁷ C.F. Maguire,⁶⁹ Y.I. Makdisi,⁶ M. Makek,^{71,74} A. Malakhov,³² M.D. Malik,⁵¹ A. Manion,⁶⁵ V.I. Manko,³⁶ E. Mannel,^{7,14} Y. Mao,^{56,58} H. Masui,⁶⁸ F. Matathias,¹⁴ M. McCumber,^{41,65} P.L. McGaughey,⁴¹ D. McGlinchey,^{13,21} C. McKinney,²⁷ N. Means,⁶⁵ A. Meles,⁵² M. Mendoza,⁸ B. Meredith,^{14,27} Y. Miake,⁶⁸ T. Mibe,³⁴ A.C. Mignerey,⁴⁴ P. Mikeš,^{9,29} K. Miki,^{58,68} A.J. Miller,¹ A. Milov,^{7,71} D.K. Mishra,⁴ M. Mishra,³ J.T. Mitchell,⁷ S. Miyasaka,^{58,67} S. Mizuno,^{58,68} A.K. Mohanty,⁴ P. Montuenga,²⁷ H.J. Moon,⁴⁹ T. Moon,⁷³ Y. Morino,¹² A. Morreale,⁸ D.P. Morrison,^{7,†} T.V. Moukhanova,³⁶ T. Murakami,^{37,58} J. Murata,^{58,60} A. Mwai,⁶⁴ S. Nagamiya,^{34,58} J.L. Nagle,^{13,‡} M. Naglis,⁷¹ M.I. Nagy,^{18,72} I. Nakagawa,^{58,59} H. Nakagomi,^{58,68} Y. Nakamiya,²⁴ K.R. Nakamura,^{37,58} T. Nakamura,^{34,58} K. Nakano,^{58,67} S. Nam,¹⁹ C. Nattrass,⁶⁶ P.K. Netrakanti,⁴ J. Newby,⁴⁰ M. Nguyen,⁶⁵ M. Nihashi,^{24,58} T. Niida,⁶⁸ R. Nouicer,^{7,59} N. Novitzky,³³ A.S. Nyanin,³⁶ C. Oakley,²² E. O’Brien,⁷ S.X. Oda,¹² C.A. Ogilvie,³⁰ M. Oka,⁶⁸ K. Okada,⁵⁹ Y. Onuki,⁵⁸ J.D. Orjuela Koop,¹³ A. Oskarsson,⁴³ M. Ouchida,^{24,58} H. Ozaki,⁶⁸ K. Ozawa,^{12,34} R. Pak,⁷ V. Pantuev,^{28,65} V. Papavassiliou,⁵² I.H. Park,¹⁹ J. Park,⁶³ S. Park,⁶³ S.K. Park,³⁵ W.J. Park,³⁵ S.F. Pate,⁵² L. Patel,²² M. Patel,³⁰ H. Pei,³⁰ J.-C. Peng,²⁷ H. Pereira,¹⁶

D.V. Perepelitsa,^{7, 14} G.D.N. Perera,⁵² V. Peresedov,³² D.Yu. Peressouko,³⁶ J. Perry,³⁰ R. Petti,⁶⁵ C. Pinkenburg,⁷ R. Pinson,¹ R.P. Pisani,⁷ M. Proissl,⁶⁵ M.L. Purschke,⁷ A.K. Purwar,⁴¹ H. Qu,²² J. Rak,³³ A. Rakotozafindrabe,³⁸ I. Ravinovich,⁷¹ K.F. Read,^{54, 66} S. Rembeczki,²⁰ K. Reygers,⁴⁷ D. Reynolds,⁶⁴ V. Riabov,⁵⁷ Y. Riabov,⁵⁷ E. Richardson,⁴⁴ N. Riveli,⁵³ D. Roach,⁶⁹ G. Roche,⁴² S.D. Rolnick,⁸ M. Rosati,³⁰ C.A. Rosen,¹³ S.S.E. Rosendahl,⁴³ P. Rosnet,⁴² Z. Rowan,⁵ J.G. Rubin,⁴⁶ P. Rukoyatkin,³² P. Ružička,²⁹ B. Sahlmueller,^{47, 65} N. Saito,³⁴ T. Sakaguchi,⁷ K. Sakashita,^{58, 67} H. Sako,³¹ V. Samsonov,⁵⁷ S. Sano,^{12, 70} M. Sarsour,²² S. Sato,³¹ T. Sato,⁶⁸ S. Sawada,³⁴ B. Schaefer,⁶⁹ B.K. Schmoll,⁶⁶ K. Sedgwick,⁸ J. Seele,^{13, 59} R. Seidl,^{27, 58, 59} A.Yu. Semenov,³⁰ A. Sen,⁶⁶ R. Seto,⁸ P. Sett,⁴ A. Sexton,⁴⁴ D. Sharma,^{65, 71} I. Shein,²⁶ T.-A. Shibata,^{58, 67} K. Shigaki,²⁴ M. Shimomura,^{30, 68} K. Shoji,^{37, 58} P. Shukla,⁴ A. Sickles,⁷ C.L. Silva,^{30, 41, 62} D. Silvermyr,⁵⁴ C. Silvestre,¹⁶ K.S. Sim,³⁵ B.K. Singh,³ C.P. Singh,³ V. Singh,³ M. Slunečka,⁹ R.A. Soltz,⁴⁰ W.E. Sondheim,⁴¹ S.P. Sorensen,⁶⁶ I.V. Sourikova,⁷ N.A. Sparks,¹ P.W. Stankus,⁵⁴ E. Stenlund,⁴³ M. Stepanov,⁴⁵ S.P. Stoll,⁷ T. Sugitate,²⁴ A. Sukhanov,⁷ T. Sumita,⁵⁸ J. Sun,⁶⁵ J. Sziklai,⁷² E.M. Takagui,⁶² A. Takahara,¹² A. Taketani,^{58, 59} R. Tanabe,⁶⁸ Y. Tanaka,⁵⁰ S. Taneja,⁶⁵ K. Tanida,^{37, 58, 59, 63} M.J. Tannenbaum,⁷ S. Tarafdar,^{3, 71} A. Taranenko,⁶⁴ P. Tarján,¹⁷ H. Themann,⁶⁵ D. Thomas,¹ T.L. Thomas,⁵¹ A. Timilsina,³⁰ T. Todoroki,^{58, 68} M. Togawa,^{37, 58, 59} A. Toia,⁶⁵ L. Tomášek,²⁹ M. Tomášek,¹⁵ H. Torii,^{24, 58} M. Towell,¹ R. Towell,¹ R.S. Towell,¹ I. Tserruya,⁷¹ Y. Tsuchimoto,²⁴ C. Vale,^{7, 30} H. Valle,⁶⁹ H.W. van Hecke,⁴¹ M. Vargyas,⁷² E. Vazquez-Zambrano,¹⁴ A. Veicht,²⁷ J. Velkovska,⁶⁹ R. Vértesi,^{17, 72} A.A. Vinogradov,³⁶ M. Virius,¹⁵ V. Vrba,^{15, 29} E. Vznuzdaev,⁵⁷ X.R. Wang,⁵² D. Watanabe,²⁴ K. Watanabe,⁶⁸ Y. Watanabe,^{58, 59} Y.S. Watanabe,³⁴ F. Wei,^{30, 52} R. Wei,⁶⁴ J. Wessels,⁴⁷ S. Whitaker,³⁰ S.N. White,⁷ D. Winter,¹⁴ S. Wolin,²⁷ J.P. Wood,¹ C.L. Woody,⁷ R.M. Wright,¹ M. Wysocki,^{13, 54} B. Xia,⁵³ W. Xie,⁵⁹ L. Xue,²² S. Yalcin,⁶⁵ Y.L. Yamaguchi,^{12, 58} K. Yamaura,²⁴ R. Yang,²⁷ A. Yanovich,²⁶ J. Ying,²² S. Yokkaichi,^{58, 59} I. Yoon,⁶³ Z. You,⁵⁶ G.R. Young,⁵⁴ I. Younus,^{39, 51} I.E. Yushmanov,³⁶ W.A. Zajc,¹⁴ A. Zelenski,⁶ C. Zhang,⁵⁴ S. Zhou,¹¹ and L. Zolin³²

(PHENIX Collaboration)

¹Abilene Christian University, Abilene, Texas 79699, USA

²Department of Physics, Augustana College, Sioux Falls, South Dakota 57197, USA

³Department of Physics, Banaras Hindu University, Varanasi 221005, India

⁴Bhabha Atomic Research Centre, Bombay 400 085, India

⁵Baruch College, City University of New York, New York, New York, 10010 USA

⁶Collider-Accelerator Department, Brookhaven National Laboratory, Upton, New York 11973-5000, USA

⁷Physics Department, Brookhaven National Laboratory, Upton, New York 11973-5000, USA

⁸University of California - Riverside, Riverside, California 92521, USA

⁹Charles University, Ovocný trh 5, Praha 1, 116 36, Prague, Czech Republic

¹⁰Chonbuk National University, Jeonju, 561-756, Korea

¹¹Science and Technology on Nuclear Data Laboratory, China Institute of Atomic Energy, Beijing 102413, P. R. China

¹²Center for Nuclear Study, Graduate School of Science, University of Tokyo, 7-3-1 Hongo, Bunkyo, Tokyo 113-0033, Japan

¹³University of Colorado, Boulder, Colorado 80309, USA

¹⁴Columbia University, New York, New York 10027 and Nevis Laboratories, Irvington, New York 10533, USA

¹⁵Czech Technical University, Zikova 4, 166 36 Prague 6, Czech Republic

¹⁶Dapnia, CEA Saclay, F-91191, Gif-sur-Yvette, France

¹⁷Debrecen University, H-4010 Debrecen, Egyetem tér 1, Hungary

¹⁸ELTE, Eötvös Loránd University, H - 1117 Budapest, Pázmány P. s. 1/A, Hungary

¹⁹Ewha Womans University, Seoul 120-750, Korea

²⁰Florida Institute of Technology, Melbourne, Florida 32901, USA

²¹Florida State University, Tallahassee, Florida 32306, USA

²²Georgia State University, Atlanta, Georgia 30303, USA

²³Hanyang University, Seoul 133-792, Korea

²⁴Hiroshima University, Kagamiyama, Higashi-Hiroshima 739-8526, Japan

²⁵Department of Physics and Astronomy, Howard University, Washington, DC 20059, USA

²⁶IHEP Protvino, State Research Center of Russian Federation, Institute for High Energy Physics, Protvino, 142281, Russia

²⁷University of Illinois at Urbana-Champaign, Urbana, Illinois 61801, USA

²⁸Institute for Nuclear Research of the Russian Academy of Sciences, prospekt 60-letiya Oktyabrya 7a, Moscow 117312, Russia

²⁹Institute of Physics, Academy of Sciences of the Czech Republic, Na Slovance 2, 182 21 Prague 8, Czech Republic

³⁰Iowa State University, Ames, Iowa 50011, USA

³¹Advanced Science Research Center, Japan Atomic Energy Agency, 2-4

Shirakata Shirane, Tokai-mura, Naka-gun, Ibaraki-ken 319-1195, Japan

³²Joint Institute for Nuclear Research, 141980 Dubna, Moscow Region, Russia

³³Helsinki Institute of Physics and University of Jyväskylä, P.O.Box 35, FI-40014 Jyväskylä, Finland

³⁴KEK, High Energy Accelerator Research Organization, Tsukuba, Ibaraki 305-0801, Japan

³⁵Korea University, Seoul, 136-701, Korea

- ³⁶Russian Research Center “Kurchatov Institute”, Moscow, 123098 Russia
³⁷Kyoto University, Kyoto 606-8502, Japan
³⁸Laboratoire Leprince-Ringuet, Ecole Polytechnique, CNRS-IN2P3, Route de Saclay, F-91128, Palaiseau, France
³⁹Physics Department, Lahore University of Management Sciences, Lahore, Pakistan
⁴⁰Lawrence Livermore National Laboratory, Livermore, California 94550, USA
⁴¹Los Alamos National Laboratory, Los Alamos, New Mexico 87545, USA
⁴²LPC, Université Blaise Pascal, CNRS-IN2P3, Clermont-Fd, 63177 Aubiere Cedex, France
⁴³Department of Physics, Lund University, Box 118, SE-221 00 Lund, Sweden
⁴⁴University of Maryland, College Park, Maryland 20742, USA
⁴⁵Department of Physics, University of Massachusetts, Amherst, Massachusetts 01003-9337, USA
⁴⁶Department of Physics, University of Michigan, Ann Arbor, Michigan 48109-1040, USA
⁴⁷Institut für Kernphysik, University of Muenster, D-48149 Muenster, Germany
⁴⁸Muhlenberg College, Allentown, Pennsylvania 18104-5586, USA
⁴⁹Myongji University, Yongin, Kyonggido 449-728, Korea
⁵⁰Nagasaki Institute of Applied Science, Nagasaki-shi, Nagasaki 851-0193, Japan
⁵¹University of New Mexico, Albuquerque, New Mexico 87131, USA
⁵²New Mexico State University, Las Cruces, New Mexico 88003, USA
⁵³Department of Physics and Astronomy, Ohio University, Athens, Ohio 45701, USA
⁵⁴Oak Ridge National Laboratory, Oak Ridge, Tennessee 37831, USA
⁵⁵IPN-Orsay, Université Paris Sud, CNRS-IN2P3, BP1, F-91406, Orsay, France
⁵⁶Peking University, Beijing 100871, P. R. China
⁵⁷PNPI, Petersburg Nuclear Physics Institute, Gatchina, Leningrad region, 188300, Russia
⁵⁸RIKEN Nishina Center for Accelerator-Based Science, Wako, Saitama 351-0198, Japan
⁵⁹RIKEN BNL Research Center, Brookhaven National Laboratory, Upton, New York 11973-5000, USA
⁶⁰Physics Department, Rikkyo University, 3-34-1 Nishi-Ikebukuro, Toshima, Tokyo 171-8501, Japan
⁶¹Saint Petersburg State Polytechnic University, St. Petersburg, 195251 Russia
⁶²Universidade de São Paulo, Instituto de Física, Caixa Postal 66318, São Paulo CEP05315-970, Brazil
⁶³Department of Physics and Astronomy, Seoul National University, Seoul, Korea
⁶⁴Chemistry Department, Stony Brook University, SUNY, Stony Brook, New York 11794-3400, USA
⁶⁵Department of Physics and Astronomy, Stony Brook University, SUNY, Stony Brook, New York 11794-3800, USA
⁶⁶University of Tennessee, Knoxville, Tennessee 37996, USA
⁶⁷Department of Physics, Tokyo Institute of Technology, Oh-okayama, Meguro, Tokyo 152-8551, Japan
⁶⁸Institute of Physics, University of Tsukuba, Tsukuba, Ibaraki 305, Japan
⁶⁹Vanderbilt University, Nashville, Tennessee 37235, USA
⁷⁰Waseda University, Advanced Research Institute for Science and Engineering, 17 Kikui-cho, Shinjuku-ku, Tokyo 162-0044, Japan
⁷¹Weizmann Institute, Rehovot 76100, Israel
⁷²Institute for Particle and Nuclear Physics, Wigner Research Centre for Physics, Hungarian Academy of Sciences (Wigner RCP, RMKI) H-1525 Budapest 114, POBox 49, Budapest, Hungary
⁷³Yonsei University, IPAP, Seoul 120-749, Korea
⁷⁴University of Zagreb, Faculty of Science, Department of Physics, Bijenička 32, HR-10002 Zagreb, Croatia

(Dated: August 14, 2019)

Two-pion interferometry measurements in d +Au and Au+Au collisions at $\sqrt{s_{NN}} = 200$ GeV are used to extract and compare the Gaussian source radii R_{out} , R_{side} , and R_{long} , which characterize the space-time extent of the emission sources. The comparisons, which are performed as a function of collision centrality and the mean transverse momentum for pion pairs, indicate strikingly similar patterns for the d +Au and Au+Au systems. They also indicate a linear dependence of R_{side} on the initial transverse geometric size \bar{R} , as well as a smaller freeze-out size for the d +Au system. These patterns point to the important role of final-state rescattering effects in the reaction dynamics of d +Au collisions.

PACS numbers: 25.75.Dw

Recent measurements for hadrons emitted in d +Au collisions ($\sqrt{s_{NN}} = 200$ GeV) at the Relativistic Heavy Ion Collider [1, 2], and in p +Pb collisions ($\sqrt{s_{NN}} = 5.02$ TeV) at the Large Hadron Collider [3–8], have indicated a surprising ridge structure in two-dimensional correlations in relative pseudorapidity ($\Delta\eta$) and azimuthal angle ($\Delta\phi$). Elucidation of the origin of these long-range correlations should advance the current understanding

of the very early-time dynamics of the matter produced in hadron nucleus (p + A and d + A) and nucleus nucleus (A + A) collisions [9–12].

Two successful approaches are currently being employed to study long-range correlations. The Color Glass Condensate (CGC) approach accounts for these correlations via an enhancement of interference diagrams in the saturation regime [10, 13]. The viscous hydrodynamical

approach [9, 14–18] accounts for the same correlations via collective harmonic flow. Thus, it is presently not clear whether the long-range ridge, observed in $d+Au$ and $p+Pb$ collisions, stems from (i) the final-state effects inherent in a hydrodynamical description, (ii) the initial-state effects driven by the correlations of gluons already present in the nucleon and nuclear wave functions or (iii) an interplay between these two mechanisms.

Interferometry measurements of the space-time extent of the emitting sources produced in $A+A$ collisions indicate characteristic patterns (as a function of collision centrality and the mean transverse momentum k_T , of particle pairs) which serve as a “fingerprint” for collective expansion [19–23]. Thus, it might be expected that similar measurements for $d+A$ and $p+A$ collisions could provide an important avenue to independently constrain the role of final-state interactions in the reaction dynamics for these systems [15, 24]. An observed similarity between the characteristic patterns for the space-time extent of $A+A$ and $d+A$ (or $p+A$) collisions would give a strong indication for the importance of final-state rescattering effects in $d+A$ and $p+A$ collisions.

In this Letter, we use the interferometry technique of Hanbury Brown and Twiss (HBT) [25] to perform detailed differential measurements of two-pion correlation functions [19–23, 26–29] in $d+Au$ and $Au+Au$ collisions at $\sqrt{s_{NN}} = 200$ GeV. In turn, these correlation functions are used to extract and study the HBT radii which characterize the space-time extent of the emission sources for the two systems. We find striking similarities in the detailed dependence of the HBT radii for both systems on collision centrality, transverse system-size, and k_T , which point to the importance of final state rescattering effects in the reaction dynamics of $d+Au$ collisions.

The present analysis uses the data recorded by the PHENIX experiment during 2007 and 2008. The collision vertex z (along the beam axis) was constrained to $|z| < 30$ cm of the nominal crossing point. Collision centrality was determined from the charge distribution measured in the beam-beam counters, which span the pseudorapidity range $3.0 < |\eta| < 3.9$ [30]. Track and momentum reconstruction for charged particles were performed by combining hits from the drift chambers (DC) and pad chambers in the PHENIX central spectrometers ($|\eta| < 0.35$). Charged pions were identified by combining time-of-flight from the time-of-flight detector and the electromagnetic calorimeters (EMCal) [31] covering azimuthal angle $\Delta\phi < \pi/2$, with momentum reconstructed from the DC and pad-chamber hits in the magnetic field. Particles within 2 standard deviations of the peak for charged pions in the squared mass distribution were identified as pions for momenta up to ~ 1 GeV/ c as detailed in Ref. [32].

The two-pion correlation function is defined as the ratio $C_2(\mathbf{q}) = A(\mathbf{q})/B(\mathbf{q})$, where $A(\mathbf{q})$ is the measured distribution of the relative momentum difference

$\mathbf{q} = \mathbf{p}_2 - \mathbf{p}_1$ between particle pairs with momenta \mathbf{p}_1 and \mathbf{p}_2 ; $B(\mathbf{q})$ is the so-called background distribution, obtained from particle pairs in which each particle is selected from a different event but with similar event centralities, vertex positions, and charge sign. The relative momentum \mathbf{q} is calculated in the longitudinally co-moving system, where the longitudinal pair momentum is zero. It is also decomposed into its three components, q_{out} , q_{side} , and q_{long} , following the Bertsch–Pratt convention [33, 34]. That is, the “out” axis points along the pair transverse momentum, the “side” axis is perpendicular to the out axis in the transverse plane, and the “long” axis points along the beam.

Track merging and track splitting [20, 21] were suppressed via pair selection cuts in the DC and the EMCal. Correlation functions were studied as a function of collision centrality, as well as for different pion-pair transverse momenta $k_T = |\mathbf{p}_{T,1} + \mathbf{p}_{T,2}|/2$ or transverse mass $m_T = \sqrt{(k_T^2 + m_\pi^2)}$, where m_π is the pion mass.

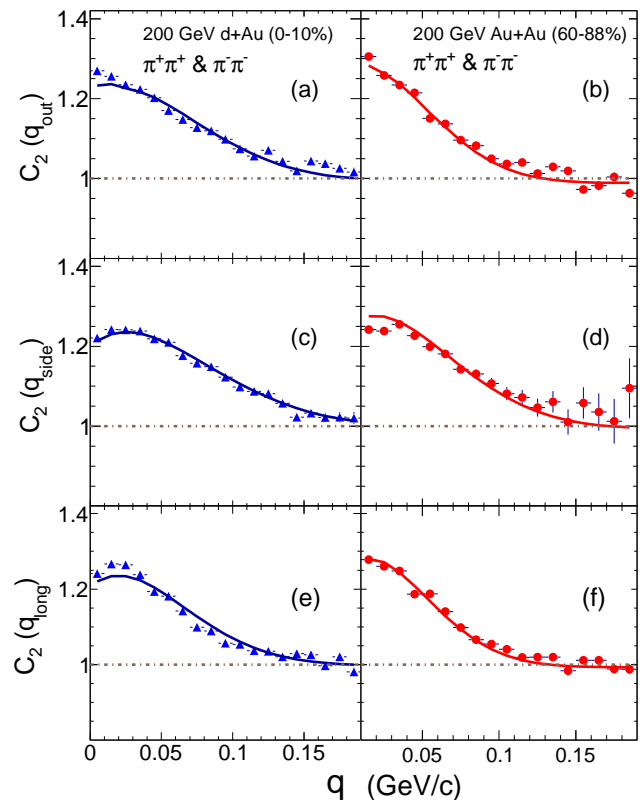


FIG. 1. (Color online) Slices of the three-dimensional two-pion ($\pi^+\pi^+$ and $\pi^-\pi^-$) correlation functions for central $d+Au$ collisions (left panels) and peripheral $Au+Au$ collisions for $0.2 < k_T < 0.7$ GeV/ c ($\langle k_T \rangle = 0.39$ GeV/ c). These centrality selections give similar N_{part} values for the two systems. The curves represent fits to the correlation function (see text).

Figure 1 shows a representative set of slices from the three-dimensional two-pion correlation functions for cen-

tral (0%–10%) d +Au and peripheral (60%–88%) Au+Au collisions for $0.2 < k_T < 0.7$ GeV/ c ($\langle k_T \rangle = 0.39$ GeV/ c). They all show the familiar Bose–Einstein enhancement peak at low q , as well as the expected difference in the peak widths for d +Au and Au+Au. The latter reflects the difference in the emission source sizes for the d +Au and Au+Au systems. Note that these centrality selections give similar values for the number of participants ($N_{\text{part}} = 16.7 \pm 1.1$ and 15.7 ± 1.6), but different values for the transverse geometric size ($\bar{R} = 0.44 \pm 0.02$ fm and 0.71 ± 0.06 fm) for d +Au and Au+Au, respectively.

A similar set of correlation functions was extracted for several centralities to facilitate detailed comparisons of the d +Au and Au+Au emission sources as a function of N_{part} , \bar{R} and k_T . Monte Carlo Glauber (MC-Glauber) calculations [30, 35, 36] were used to compute N_{part} and \bar{R} as a function of collision centrality, from the two-dimensional profile of the density of point-like sources in the transverse plane $\rho_s(\mathbf{r}_\perp)$, where $1/\bar{R} = \sqrt{(1/\sigma_x^2 + 1/\sigma_y^2)}$, with σ_x and σ_y the respective root-mean-square widths of the density distributions [37]. The systematic uncertainties for these geometric quantities, obtained via variation of the MC-Glauber model parameters, are less than 10% [30].

To aid the comparisons, the measured correlation functions were fitted with the following expression (in which cross-terms are assumed to be negligible) which accounts for the Bose–Einstein enhancement and the Coulomb interaction between pion pairs [38, 39]:

$$C_2(\mathbf{q}) = N[(\lambda(1 + G(\mathbf{q}))F_c + (1 - \lambda)), \\ G(\mathbf{q}) \cong \exp(-R_{\text{side}}^2 q_{\text{side}}^2 - R_{\text{out}}^2 q_{\text{out}}^2 - R_{\text{long}}^2 q_{\text{long}}^2), \quad (1)$$

where N is a normalization factor, λ is the correlation strength, F_c is the Coulomb correction factor [39] evaluated with the Coulomb wave function, and R_{out} , R_{side} , and R_{long} are the Gaussian HBT radii which characterize the emission source. R_{side} and R_{long} are related to the transverse and longitudinal size of the source; R_{out} includes additional effects from the emission duration.

Excellent fits to the correlation functions for the d +Au and Au+Au systems were obtained and cross-checked to confirm agreement with our earlier measurements for Au+Au and d +Au collisions [20, 21, 40]. The fit parameters for $\pi^+\pi^+$ and $\pi^-\pi^-$ pairs were also found to agree within statistical errors; the data for $\pi^+\pi^+$ and $\pi^-\pi^-$ were therefore combined. The systematic uncertainties for the fits were estimated via variations of the cuts used to generate the correlation functions (single track cuts, pair selection cuts and particle identification cuts). Typical values of the systematic uncertainties are 5.0%(7.5%) for the extracted values of R_{out} , R_{side} , and R_{long} for Au+Au(d +Au) and do not exceed 7.5%(10.0%).

Figure 2 shows a comparison of the m_T dependence of R_{out} , R_{side} , and R_{long} for 0%–10% central d +Au and 60%–88% central Au+Au collisions, i.e. similar values of

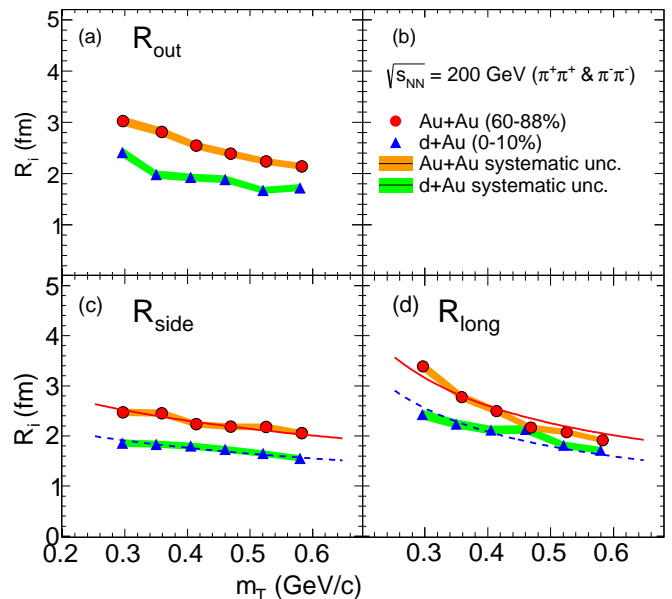


FIG. 2. (Color online) Comparison of the m_T dependence of R_{out} , R_{side} , and R_{long} for 0%–10% central d +Au and 60%–88% central Au+Au collisions. The solid and dashed curves in panels (c) and (d) indicate fits to the data (see text). The color bands indicate the systematic uncertainties.

N_{part} . The radii for d +Au and Au+Au show a decreasing trend with increasing values of m_T . The R_{out} radius is also comparable to R_{side} (for both systems) and the m_T dependence of the ratio $R_{\text{out}}/R_{\text{side}}$ is flat or gently decreasing, as shown in Fig. 3(a). The same trends have been observed in central Au+Au and Pb+Pb collisions [20–23, 28] and are commonly identified as a characteristic signature for the expansion of an emitting source of short emission duration, driven by final-state rescattering effects [41]. Therefore, we interpret the similarity between the observed patterns for Au+Au and d +Au in Figs. 2 and 3, as an indication for final-state rescattering effects in the reaction dynamics for d +Au.

The curves in Fig. 2 show blast wave expansion model inspired fits to R_{side} and R_{long} with fit functions [42, 43]:

$$R_{\text{side}} = R_{\text{geom}} / \sqrt{(1 + \beta^2(m_T/T))}, \quad (2)$$

$$R_{\text{long}} = \tau_0 \sqrt{(T/m_T)[(K_2(m_T/T))/(K_1(m_T/T))]}, \quad (3)$$

where R_{geom} is the geometrical radius at freeze-out and

TABLE I. Fit parameters

	d +Au	Au+Au
τ_0 (fm/c)	$3.2 \pm 0.04 \pm 0.4$ (syst)	$3.8 \pm 0.04 \pm 0.3$ (syst)
χ^2/ndf	26/5	24/5
R_{geom} (fm)	$2.2 \pm 0.03 \pm 0.2$ (syst)	$2.8 \pm 0.03 \pm 0.2$ (syst)
χ^2/ndf	6/5	4/5

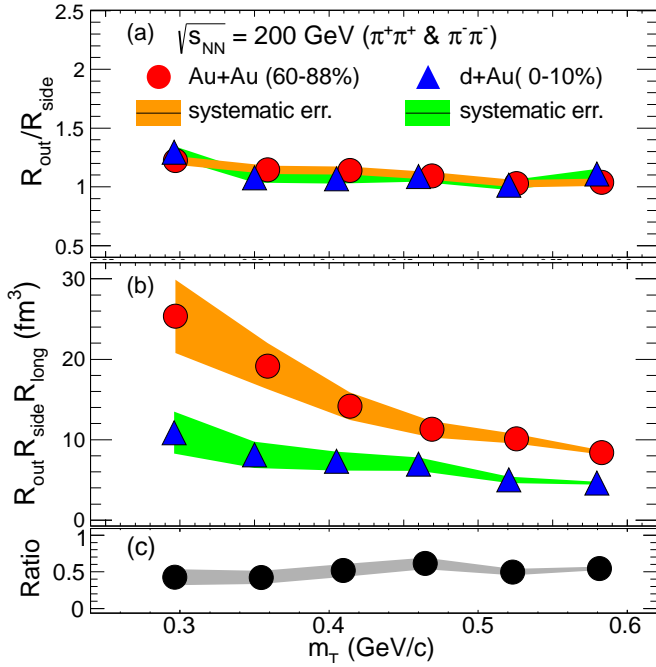


FIG. 3. (Color online) Comparison of the m_T dependence of; (a) the ratio R_{out}/R_{side} ; (b) the freeze-out volume, and (c) the ratio of the freeze-out volumes, for 0%–10% central $d+Au$ and 60%–88% central $Au+Au$ collisions.

τ_0 is the expansion time. The requisite freeze-out temperatures ($T = 0.118 \pm 0.02$ and 0.123 ± 0.02 GeV) and expansion velocities ($\langle\beta\rangle = 0.42 \pm 0.03$ and $0.38 \pm 0.08 c$) for $d+Au$ and $Au+Au$ (respectively), are interpolated values obtained from a blast wave fit to the p_T spectra for identified charged hadrons [44]; K_1 and K_2 are modified Bessel functions. The fit results are summarized in Table I; they suggest a smaller transverse freeze-out size for the $d+Au$ emitting source.

Figure 3(b) further illustrates the difference via the m_T dependence of the freeze-out volume, evaluated as the product ($R_{out} \times R_{side} \times R_{long}$) for the same $\langle N_{part} \rangle$ values employed in Fig. 2. The magnitudes of the freeze-out volumes for $Au+Au$ are larger. However, within uncertainties, the fall-off with increasing m_T is comparable for $d+Au$ and $Au+Au$ as shown by the ratio in Fig. 3(c).

Detailed comparisons were also made as a function of collision centrality. Figs. 4(a-c) show one such comparison of R_{out} , R_{side} , and R_{long} for $d+Au$ and $Au+Au$, as a function of $N_{part}^{1/3}$ for $\langle k_T \rangle = 0.39$ GeV/ c . The solid and dashed curves represent linear fits to the $Au+Au$ and $d+Au$ data, respectively. The data for R_{out} and R_{side} indicate a similar linear increase with $N_{part}^{1/3}$, albeit with larger magnitudes for $Au+Au$. An apparent slope difference between $d+Au$ and $Au+Au$ for R_{long} (Fig. 4c), could be the result of a difference in the longitudinal dynamics for the two systems. The representative plot of R_{side} vs. $(dN/d\eta)^{1/3}$ shown in Fig. 4(d), indicates that

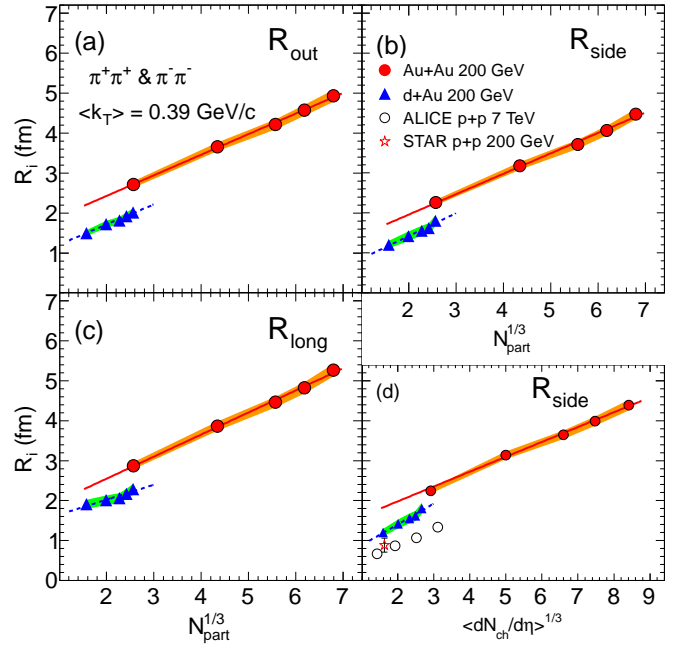


FIG. 4. (Color online) (a,b,c) HBT radii (R_{out} , R_{side} and R_{long}) vs. $N_{part}^{1/3}$ for $Au+Au$ and $d+Au$ collisions. (d) R_{side} vs $\langle dN_{ch}/d\eta \rangle^{1/3}$ for $Au+Au$, $d+Au$ and $p+p$ [45, 46] collisions. Results are shown for $\langle k_T \rangle = 0.39$ GeV/ c . The solid and dashed curves represent linear fits to the $Au+Au$ and $d+Au$ data, respectively. The color bands indicate the systematic uncertainties.

the HBT radii for $d+Au$ do follow the linear dependence previously observed for $A+A$ and $p+p$ collisions [46], but with separate magnitudes for each system.

The dependencies shown in Figs. 4(a-c) suggest that the pattern of a strong correlation between the transverse freeze-out size and the initial geometric size, is similar for both $d+Au$ and $Au+Au$. They also suggest that at $\sqrt{s_{NN}} = 200$ GeV, the change in the transverse expansion rates with centrality (defined by N_{part}) is similar for central $d+Au$ and peripheral $Au+Au$ collisions.

In some models [11, 47, 48], the expansion time is proportional to the initial geometric size $\tau \propto \bar{R}$. Therefore, \bar{R} might be expected to be a more natural scaling variable for the HBT radii of expanding systems. The detailed dependencies of R_{side} on \bar{R} are compared in Fig. 5(a) for $d+Au$ and $Au+Au$ collisions at $\sqrt{s_{NN}} = 200$ GeV, and $Pb+Pb$ collisions at $\sqrt{s_{NN}} = 2.76$ TeV for $\langle k_T \rangle \sim 0.4$ GeV/ c . Fig. 5(b) shows a similar dependence for recent R_{inv} measurements for $p+Pb$ and $Pb+Pb$ collisions [49]. The comparisons indicate that R_{side} and R_{inv} scale linearly with \bar{R} for all of these systems. This pattern is consistent with the observed $1/\bar{R}$ scaling of collective anisotropic flow [12, 47]. The dashed curves in Figs. 5(a) and (b) are linear fits to the $d+Au$ and $Au+Au$ ($p+Pb$ and $Pb+Pb$) data sets; they suggest similar slopes for $d+Au$ and $Au+Au$ ($p+Pb$ and $Pb+Pb$). The fit to

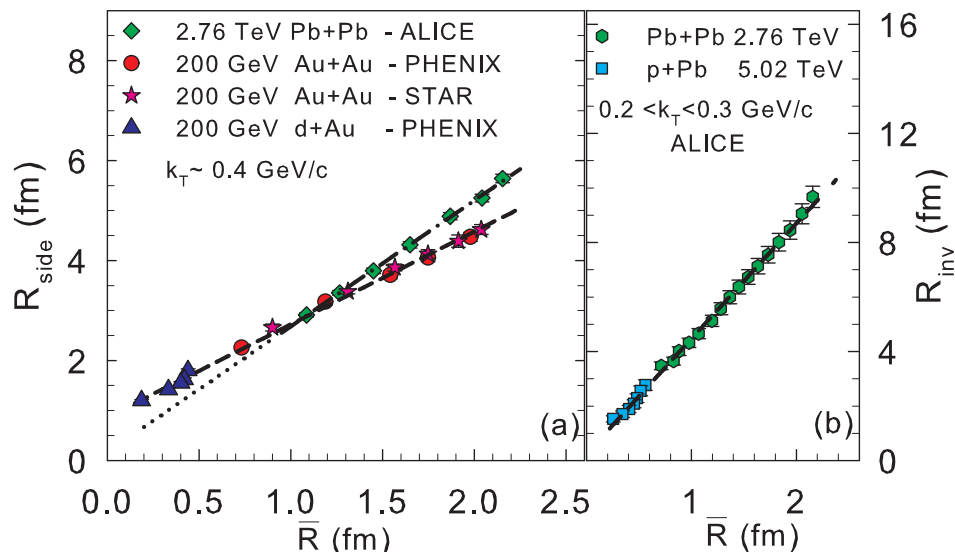


FIG. 5. (Color online) (a) R_{side} vs. \bar{R} , for $\langle k_T \rangle \approx 0.4$ GeV/c for d +Au, Au+Au and Pb+Pb collisions as indicated. (b) R_{inv} vs. \bar{R} for p +Pb and Pb+Pb collisions. The ALICE and STAR data are taken from Refs. [23, 49] and [22] respectively. Systematic uncertainties are 5.0%(7.5%) for Au+Au(d +Au). The dashed curves in a (b) represents a linear fit to the Au+Au and d +Au (p +Pb and Pb+Pb) data sets. The dotted curve is an extrapolation of the dashed-dot curve.

the Pb+Pb data in Figs. 5(a) (dotted curve) indicates a larger slope for Pb+Pb collisions at the much higher energy of $\sqrt{s_{NN}} = 2.76$ TeV, where the expansion rate is expected to be larger. The observed dependencies of R_{side} and R_{inv} on \bar{R} reinforce our earlier inferences that the final-state rescattering effects, which are known to play a dominant role in Au+Au and Pb+Pb collisions, also play an important role in d +Au and p +Pb collisions.

In summary, we have presented detailed comparisons of HBT radii, which emphasize trends commonly associated with hydrodynamic-like expansion. Excellent agreement is found between the patterns for the d +Au and Au+Au systems. The radii extracted for the two systems at similar $\langle N_{\text{part}} \rangle$ show similar dependencies on m_T , which indicate a smaller geometric size (at freeze-out) for the emitting source in d +Au collisions. The R_{side} and R_{inv} radii for different systems show scaling with the initial transverse size \bar{R} , across several collision energies, which is indicative of hydrodynamic-like collective expansion driven by final-state rescattering effects. An investigation of the interesting possibility of a similar pattern in high multiplicity p + p events is deferred to a future study. Our present findings, which support the view that the expansion dynamics for d +Au and Au+Au (p +Pb and Pb+Pb) are similar, constitute a significant contribution towards a more comprehensive understanding of the very early-time dynamics of the matter produced in hadronic collisions.

ACKNOWLEDGMENTS

We thank the staff of the Collider-Accelerator and Physics Departments at Brookhaven National Laboratory and the staff of the other PHENIX participating institutions for their vital contributions. We acknowledge support from the Office of Nuclear Physics in the Office of Science of the Department of Energy, the National Science Foundation, Abilene Christian University Research Council, Research Foundation of SUNY, and Dean of the College of Arts and Sciences, Vanderbilt University (U.S.A), Ministry of Education, Culture, Sports, Science, and Technology and the Japan Society for the Promotion of Science (Japan), Conselho Nacional de Desenvolvimento Científico e Tecnológico and Fundação de Amparo à Pesquisa do Estado de São Paulo (Brazil), Natural Science Foundation of China (P. R. China), Ministry of Education, Youth and Sports (Czech Republic), Centre National de la Recherche Scientifique, Commissariat à l'Énergie Atomique, and Institut National de Physique Nucléaire et de Physique des Particules (France), Bundesministerium für Bildung und Forschung, Deutscher Akademischer Austausch Dienst, and Alexander von Humboldt Stiftung (Germany), Hungarian National Science Fund, OTKA (Hungary), Department of Atomic Energy and Department of Science and Technology (India), Israel Science Foundation (Israel), National Research Foundation of Korea of the Ministry of Science, ICT, and Future Planning (Korea), Physics Department, Lahore University of Management Sciences (Pakistan), Ministry of Education and Science, Russian Academy of Sciences, Federal Agency of Atomic Energy

(Russia), VR and Wallenberg Foundation (Sweden), the U.S. Civilian Research and Development Foundation for the Independent States of the Former Soviet Union, the US-Hungarian Fulbright Foundation for Educational Exchange, and the US-Israel Binational Science Foundation.

* Deceased

† PHENIX Co-Spokesperson: morrison@bnl.gov

‡ PHENIX Co-Spokesperson: jamie.nagle@colorado.edu

- [1] A. Adare *et al.* (PHENIX Collaboration), (to be published).
- [2] A. Adare *et al.* (PHENIX Collaboration), Phys. Rev. Lett. **111**, 202301 (2013).
- [3] S. Chatrchyan *et al.* (CMS Collaboration), Phys. Lett. B **718**, 795 (2013).
- [4] B. Abelev *et al.* (ALICE Collaboration), Phys. Lett. B **719**, 29 (2013).
- [5] G. Aad *et al.* (ATLAS Collaboration), Phys. Rev. Lett. **110**, 182302 (2013).
- [6] G. Aad *et al.* (ATLAS Collaboration), Phys. Lett. B **725**, 60 (2013).
- [7] S. Chatrchyan *et al.* (CMS Collaboration), Phys. Lett. B **724**, 213 (2013).
- [8] B. B. Abelev *et al.* (ALICE Collaboration), Phys. Lett. B **726**, 164 (2013).
- [9] P. Bozek, Phys. Rev. C **85**, 014911 (2012).
- [10] K. Dusling and R. Venugopalan, Phys. Rev. Lett. **108**, 262001 (2012).
- [11] E. Shuryak and I. Zahed, Phys. Rev. C **88**, 044915 (2013).
- [12] R. A. Lacey, D. Reynolds, A. Taranenko, N. N. Ajitanand, J. M. Alexander, F.-H. Liu, Y. Gu, and A. Mwai, arXiv:1311.1728.
- [13] K. Dusling and R. Venugopalan, Phys. Rev. D **87**, 094034 (2013).
- [14] P. Bozek and W. Broniowski, Phys. Rev. C **88**, 014903 (2013).
- [15] A. Bzdak, B. Schenke, P. Tribedy, and R. Venugopalan, Phys. Rev. C **87**, 064906 (2013).
- [16] G.-Y. Qin and B. Muller, arXiv:1306.3439.
- [17] K. Werner, M. Bleicher, B. Guiot, I. Karpenko, and T. Pierog, arXiv:1307.4379.
- [18] P. Bozek, W. Broniowski, and G. Torrieri, Phys. Rev. Lett. **111**, 172303 (2013).
- [19] M. A. Lisa, S. Pratt, R. Soltz, and U. Wiedemann, Ann. Rev. Nucl. Part. Sci. **55**, 357 (2005).
- [20] S. Adler *et al.* (PHENIX Collaboration), Phys. Rev. Lett. **93**, 152302 (2004).
- [21] S. Afanasiev *et al.* (PHENIX Collaboration), Phys. Rev. Lett. **100**, 232301 (2008).
- [22] J. Adams *et al.* (STAR Collaboration), Phys. Rev. C **71**, 044906 (2005).
- [23] K. Aamodt *et al.* (ALICE Collaboration), Phys. Lett. B **696**, 328 (2011).
- [24] P. Bozek and W. Broniowski, Phys. Lett. B **720**, 250 (2013).
- [25] R. H. Brown and R. Q. Twiss, Nature **178**, 1046 (1956).
- [26] W. A. Zajc, J. A. Bistirlich, R. R. Bossingham, H. R. Bowman, C. W. Clawson, *et al.*, Phys. Rev. C **29**, 2173 (1984).
- [27] S. Pratt, Phys. Rev. Lett. **53**, 1219 (1984).
- [28] R. Ganz *et al.* (NA49 Collaboration) (1998).
- [29] A. Adare *et al.* (PHENIX Collaboration) (2014).
- [30] A. Adare *et al.* (PHENIX Collaboration), arXiv:1310.4793.
- [31] L. Aphecetche *et al.*, Nucl. Instrum. Meth. **A499**, 521 (2003).
- [32] A. Adare *et al.* (PHENIX Collaboration), Phys. Rev. C **88**, 024906 (2013).
- [33] G. F. Bertsch, Nucl. Phys. **A498**, 173C (1989).
- [34] S. Pratt, Phys. Rev. D **33**, 1314 (1986).
- [35] M. L. Miller, K. Reygers, S. J. Sanders, and P. Steinberg, Ann. Rev. Nucl. Part. Sci. **57**, 205 (2007).
- [36] R. A. Lacey, R. Wei, J. Jia, N. Ajitanand, J. M. Alexander, and A. Taranenko, Phys. Rev. C **83**, 044902 (2011).
- [37] R. Bhalerao, J.-P. Blaizot, N. Borghini, and J.-Y. Ollitrault, Phys. Lett. B **627**, 49 (2005).
- [38] M. G. Bowler, Phys. Lett. B **270**, 69 (1991).
- [39] Y. Sinyukov, R. Lednicky, S. Akkelin, J. Pluta, and B. Erasmus, Phys. Lett. B **432**, 248 (1998).
- [40] P. Chung, A. Taranenko, R. Lacey, W. Holzmann, J. Alexander, *et al.*, Nucl. Phys. A **749**, 275 (2005).
- [41] M. Herrmann and G. F. Bertsch, Phys. Rev. C **51**, 328 (1995).
- [42] S. Chapman, J. R. Nix, and U. W. Heinz, Phys. Rev. C **52**, 2694 (1995).
- [43] B. Tomasik, arXiv:nucl-th/0304079.
- [44] B. Abelev *et al.* (STAR Collaboration), Phys. Rev. C **79**, 034909 (2009).
- [45] M. Aggarwal *et al.* (STAR Collaboration), Phys. Rev. C **83**, 064905 (2011).
- [46] K. Aamodt *et al.* (ALICE Collaboration), Phys. Rev. D **84**, 112004 (2011).
- [47] R. A. Lacey, Y. Gu, X. Gong, D. Reynolds, N. N. Ajitanand, J. M. Alexander, A. Mwai, and A. Taranenko, arXiv:1301.0165.
- [48] R. A. Lacey, A. Taranenko, J. Jia, D. Reynolds, N. Ajitanand, *et al.*, Phys. Rev. Lett. **112**, 082302 (2014).
- [49] B. B. Abelev *et al.* (ALICE Collaboration), arXiv:1404.1194.